Progress In Electromagnetics Research, Vol. 120, 195–213, 2011

RF DIRECTIONAL MODULATION TECHNIQUE USING A SWITCHED ANTENNA ARRAY FOR COMMUNICATION AND DIRECTION-FINDING APPLICATIONS

T. Hong*, M.-Z. Song, and Y. Liu

College of Electronic and Information Engineering, Nanjing University of Aeronautics and Astronautics, Nanjing 210016, China

Abstract—A RF directional modulation technique using a switched antenna array is proposed for communication and direction-finding applications. The main idea is that a baseband modulation signal is transmitted by the switched antenna array. The phase center of the transmit signal is moved by the feeding line of each element from the left to the right. In this way, the data information and Doppler frequency shift information are modulated into a transmit signal constellation simultaneously. Therefore, this constellation is a scrambled constellation compared with traditional baseband modulation signal, which varies with the azimuth angle information of the receiver. For the receiver with a single antenna, a differential correlation algorithm is employed to demodulate the data information, and an azimuth angle estimation algorithm is also developed to extract the azimuth angle information from this scrambled constellation. Simulation results show that this RF directional modulation technique offers a comprehensive scheme for communication and direction-finding from the point view of RF modulation technique.

1. INTRODUCTION

In traditional wireless communication transmitter, data information is modulated at baseband and then up-converted to radio frequency (RF). The modulation RF signal goes through a power amplifier to drive a transmit antenna or antenna array. It is noteworthy that in this traditional transmitter, a receiver at the sidelobe of the transmit antenna receives the same information as the receiver

Received 12 July 2011, Accepted 22 August 2011, Scheduled 5 September 2011

* Corresponding author: Tao Hong (hongtao3223@163.com).

located at the transmit antenna's main beam. The only difference between the receive signal at different directions is the signal power. Therefore, given a high-sensitivity receiver it would be possible for a receiver at an undesired direction to eavesdrop data information. RF directional modulation technique is proposed for the physical layer secure communication in the paper [1–5], which synthesizes a digital modulation signal fully or partially in the RF portion of the transmitter. Papers [1, 2] propose a direction modulation (DM) technique using a phased array, which synthesizes the digital modulation signal in RF portion of the transmitter. The constellation points of the transmit signal maintain their positions at the desired direction but scrambled at the undesired directions. Therefore, the desired receiver can demodulate the receive signal as traditional digital modulation signal, while the undesired receivers cannot extract any useful information from the scrambled constellation. Paper [3] presents a similar DM signal transmitted by an array with pattern reconfigurable elements. Paper [4] introduces a near-field direct antenna modulation (NFDAM) technique, which forms a DM signal by two transmit beams or multiple transmit beams. Paper [5] proposes a RF directional modulation technique using a switched antenna array which combines the advantages of the DM signal with traditional spread-spectrum signal. These DM techniques cause the transmit signal to be direction-dependent. This characteristic is beneficial for physical layer secure communication without relying on upper layer data encryption. In fact, this scrambled constellation generated by RF directional modulation technique contains azimuth angle information of the receiver with respect to the transmitter. Paper [6] designs an inverse monopulse system for communication and direction-finding applications based on sum and difference beams NFDAM technique. Paper [7] proposes a multiple beams OFDM-NFDAM signal transmitted by a sparse antenna array for communication and direction-finding applications. These papers prove that the receiver can demodulate the data information and azimuth angle information from this scrambled constellation simultaneously, if a proper RF modulation technique is designed for the transmitter. Therefore, a goal of this paper is to design a RF directional modulation signal using a switched antenna array for communication and direction-finding applications.

The Doppler frequency shift information of the transmit signal contains azimuth angle information of the receiver with respect of the transmitter, if the transmitter is moved as a regular way with high-speed. Unfortunately, this assumption can hardly be held in practical scenarios. RF switches are developed to control "on-out" state of the transmit antenna with high-speed [8]. Therefore, we design a switched antenna array to simulate linear motion of the transmit antenna with high-speed in this paper. Radiation pattern synthesis is widely used to obtain shaped radiation pattern for wireless communication system and radar system [9–12]. Switched antenna array is also called time modulated linear array (TMLA) in the field of radiation pattern synthesis. In the late 1950s, "Time" as a design parameter is first proposed to suppress the sidelobes of the linear array in [13]. Researches on TMLA have followed this work for the purpose of achieving lower sidelobe level [14–23]. Papers [14–18] use differential evolution (DE) algorithm [14, 15], genetic algorithm [16] and particle swarm algorithm [17, 18] to synthesize the radiation pattern of the TMLA. Paper [19] presents a sidelobe suppression method using a TMLA with unequal element spacing. Paper [20] analyzes the TMLA using the FDTD method. Papers [21–23] propose a phase center motion technique to obtain lower sidelobe level by Doppler frequency shift effect for the TMLA. These papers focus on shaping the beam requirements and suppressing the sidelobe level. TMLA is also widely applied to airborne pulsed Doppler radar system [24], direction of arrivals (DOAs) system [25], sum and difference patterns synthesis for monopulse system [26, 27] and digital beamforming (DBF) system [28]. However, the inherent drawback of TMLA is that there are many sideband signals spaced at multiples of the modulation frequency, called sideband radiation. In [29], a closed form expression associated with the sideband power losses is obtained. SR signals may not be desirable and should be suppressed to improve the efficiency of the TMLA. Paper [30] proposes a DE algorithm to suppress the sideband radiation patterns in TMLA. Paper [31] uses half-power sub-arraying technique to reduce the sideband levels. Papers [32–34] control the harmonic radiation pattern based on the particle swarm algorithm. Paper [34] obtains the minimization of the power losses in TMLA by means of a suitable strategy based on particle swarm optimization. These researches consider that SR signals are major disadvantage of TMLA and should be suppressed or filtered from the point view of radiation pattern synthesis. The major disadvantage of TMLA mentioned above may also be used as an advantage in applications. Fundamental frequency component and first harmonic of a two-element TMLA are used in direction finding by steering the deep null on broadside direction in [35, 36]. First harmonic of a TMLA with the aid of variable-switching instants can be used in beam-steering applications [37, 38]. A multiple harmonic beamforming technique is also presented based on particle swarm algorithm in [39]. Additionally, switched architecture is considered an attractive alternative to fully adaptive arrays due to low-cost of the switched architecture because this switched architecture offers a drastic reduction in the amount of RF hardware (power amplifiers, mixers) required. Therefore, switched antenna arrays are widely used for mobile 2.4 GHz ISM applications [40], wireless senor networks [41] and WIMAX [42].

Our work in this paper is different from the aforementioned works in the following aspects: i) The switched antenna array is employed to simulate motion of the transmit antenna with high-speed which is similar to papers [21–23]. However, in this paper the Doppler frequency shift information is modulated into the transmit signal constellation for the purpose of direction-finding applications, different from papers [21–23] which utilize Doppler frequency shift effect of the phase center for the purpose of synthesizing the radiation pattern; ii) The RF directional modulation signal using a switched antenna array is proposed for communication and direction-finding applications, unlike paper [5] for the physical layer secure communication; iii) From the point view of signal modulation, each harmonic component contains the same information as the fundamental frequency component, which is useful for wireless communication. Therefore, the fundamental frequency component and all harmonic components are used to form a RF directional modulation signal, unlike the radiation pattern synthesis only using fundamental frequency component in papers [10–23], direction-finding using fundamental frequency component and first harmonic components [35, 36] and harmonic beam-steering applications [37, 38]. This characteristic of the transmit signal spectrum is similar to traditional spread-spectrum signal. Therefore, a differential correlated demodulation is employed to demodulate the data information from the scrambled constellation, unlike paper [5] which demodulates the receive signal as a traditional direct sequence spread-spectrum signal; iii) The Doppler frequency shift information of the switched antenna array is modulated into the transmit signal constellation different from papers [6, 7], which modulate the spatial parameter of the radiation pattern into the transmit signal constellation. In this way, an azimuth angle estimation algorithm is developed to extract the azimuth angle information from the scrambled constellation based on frequency measurement algorithm, unlike papers [6, 7, 26, 27, 35, 36], which are similar to monopulse system based on the amplitude-comparison algorithm using the multiple transmit beams [6, 7], sum-difference patterns [26, 27] and fundamental frequency component and first harmonic components [35, 36], respectively. The direction finding method proposed in this paper is similar to that in paper [25], which extracts the directional information from the Doppler frequency shift. However, paper [25] only considers the direction-finding applications using TMLA at the receiver based on MUSIC algorithm, unlike this paper which proposes a comprehensive scheme for communication and direction-finding using TMLA at the transmitter.

The remainder of this paper is organized as follows. Section 2 introduces the principle of RF directional modulation signal using a switched antenna array. Section 3 gives the differential correlated demodulation of the data information. Section 4 develops an azimuth angle estimation algorithm from the scrambled constellation. Finally, the communication and direction-finding performances of the RF directional modulation signal are investigated by computer simulation in Section 5.

2. THE PRINCIPLE OF RF DIRECTIONAL MODULATION TECHNIQUE USING A SWITCHED ANTENNA ARRAY

To illustrate the principle of RF directional modulation technique, a block diagram of the transmitter is designed as shown in Figure 1, which consists of data source, differential encoder, modulator, power amplifier (PA), power splitter, CPLD module, phase shifter and a switched linear array. The isotropic elements with equal space ($d = \frac{\lambda}{2}$) are numbered from 1 to H. Considering that each element is controlled by a high-speed RF switch, we can implement the moving phase center technique by high speed RF switches in the feed line of each element.

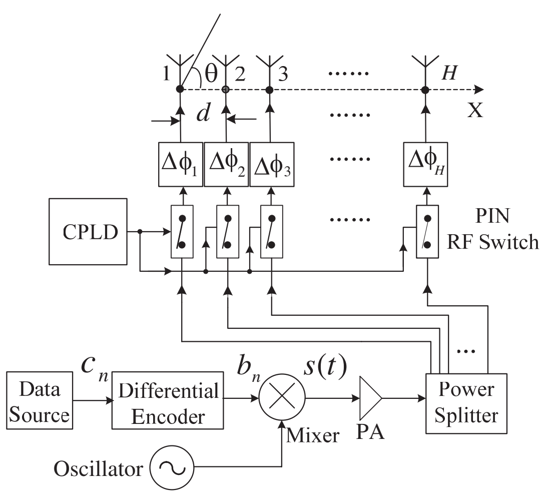

Figure 1. Block diagram of the transmitter.

2.1. Time-domain Analysis

The excitation signal for this switched antenna array is $s(t) = b_n e^{j\omega_0 t}$, where $b_n = c_n \oplus b_{n-1} \in \{+1, -1\}$ denotes the BPSK modulation symbol; $c_n \in \{+1, -1\}$ denotes the data information; $n = 1, 2, \dots, N$ denotes the nth BPSK modulation symbol in each frame signal. Firstly, a cluster of V consecutive elements ($V < H$) are switched on from the left to the right. Therefore, the switched antenna array is divided into $\frac{H}{V}$ antenna clusters and denoted by $L_m \in \{1, 2, \dots, M = \frac{H}{V}\}$, $m = 1, 2, \dots,$ M where m denotes the mth antenna cluster. Then, the cluster is electronically moved across the linear array to transmit one BPSK modulation symbol. Consider that the switching frequency f_p equals the symbol rate of the BPSK modulation signal. The duration of "on" times is the same for all switching antenna cluster. Therefore, the duration of "on" times for the mth switching antenna cluster is written as:

$$\tau_{L_m} = \tau = \frac{1}{M} T \tag{1}$$

where $T = \frac{1}{f_p}$ is the switching period. The schematic diagram of the antenna switching is shown in Figure 2 when V and M equal 1 and 7, respectively.

Supposing that the desired receiver is at the range of $[\theta_1, \theta_2]$. To direct main beam to the desired range, the phase value for each phase shifter can be calculated as follows:

$$\phi_h = -(h-1)\beta d \cos\left(\frac{\theta_1 + \theta_2}{2}\right), h = 1, 2, \dots, H \tag{2}$$

where $\beta = \frac{2\pi}{\lambda}$ denotes the propagation constant; λ denotes a wavelength; h denotes hth antenna. For example, we consider that BPSK modulation symbol period equals 7×10^{-5} s, $M = 7$ and that the desired receiver is at the range of $[40^{\circ}, 50^{\circ}]$. Figure 3 shows the phase center locus of the switched antenna array for the purpose

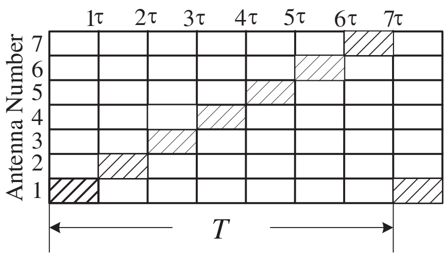

Figure 2. The schematic diagram of the antenna cluster switching.

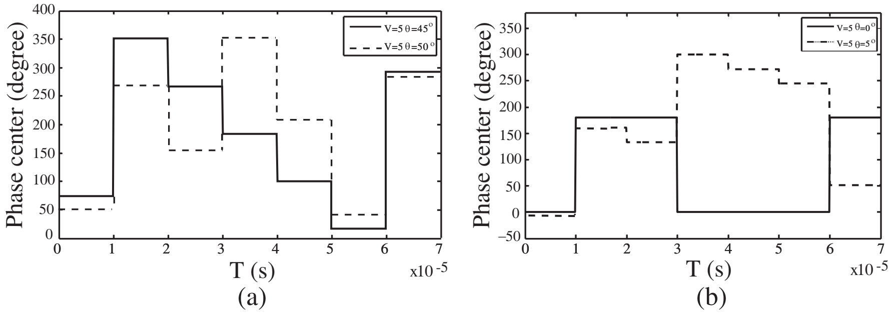

Figure 3. Phase center locus of the switched antenna array for different applications. (a) Communication and direction-finding application. (b) Secure communication application.

of: 1) physical layer secure communication application in paper [5], and 2) communication and direction-finding application in this paper, respectively. For the physical layer secure communication application, the switching scheme of the switched antenna array is according to the spreading sequence. Therefore, the phase center locus is the same as the spreading sequence at the desired direction $\theta = 0^{\circ}$, while the phase center locus is scrambled at the undesired direction $\theta = 10^{\circ}$. This characteristic is beneficial for secure communication at physical layer. For the communication and direction-finding application, the switching scheme of the switched antenna array is switched on from the left to the right. Therefore, the Doppler frequency shift information of the phase center is modulated into the transmit signal constellation, which can realize communication and direction-finding function with the desired receiver.

According to the excitation scheme mentioned above, the receive signal at the azimuth angle θ is expressed as follows:

$$r(t) = b_n \sum_{h=V(L_m-1)+1}^{h=V(L_m-1)+V} U_m(t) e^{j[\beta(h-1)d\cos\theta+\phi_h]} e^{j(\omega_0 t+\psi)} \tag{3}$$

where $\omega_0 = 2\pi f_0$ denotes the carrier radian frequency; f_0 is the carrier frequency, ψ is an random RF phase delay; m denotes mth transmit antenna cluster; $U_m(t)$ is switching function of the antenna. The expression of the switching function is expressed by Equation (4), and its schematic diagram is shown in Figure 4.

$$U_m(t) = \begin{cases} 1, & t_{0m} \leq t \leq (t_{0m}+\tau) \\ 0, & \leq t \leq t_{0m},\ (t_{0m}+\tau) \leq t \leq T \end{cases} \tag{4}$$

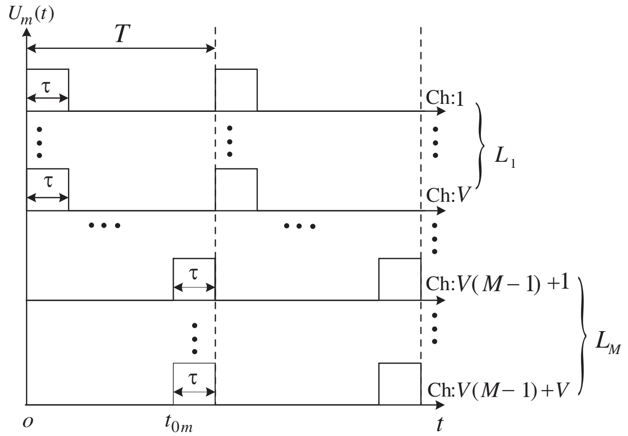

Figure 4. Schematic diagram of the switching function.

where t_{0m} denotes the switch-on time instant of the mth antenna cluster; τ is the duration of "on" times; $T = \frac{1}{f_p}$ is the switching period; f_p is the switching frequency.

2.2. Transmit Signal Constellation

According to the switching scheme mentioned above, the phase center of the switched antenna array is moved in the direction of X-axis from the left to the right. Therefore, the motion velocity of the phase center is written as:

$$v = \frac{(M-1)Vd}{T} \tag{5}$$

The Doppler frequency shift information f_d of the phase center is expressed as:

$$f_d(M, \theta, f_p) = \frac{v \cos\theta}{\lambda} = \frac{(M-1)\,V}{2} f_p \cos\theta \tag{6}$$

Considering that total phase value is expressed by ς during the period of the BPSK symbol T, we can write the relationship between ς and f_d as:

$$\varsigma = 2\pi \int_0^T f_d dt \tag{7}$$

From Equations (4) and (5), we can find that the Doppler frequency shift information of the phase center contains the azimuth angle information with respect to the transmitter. Therefore, the azimuth

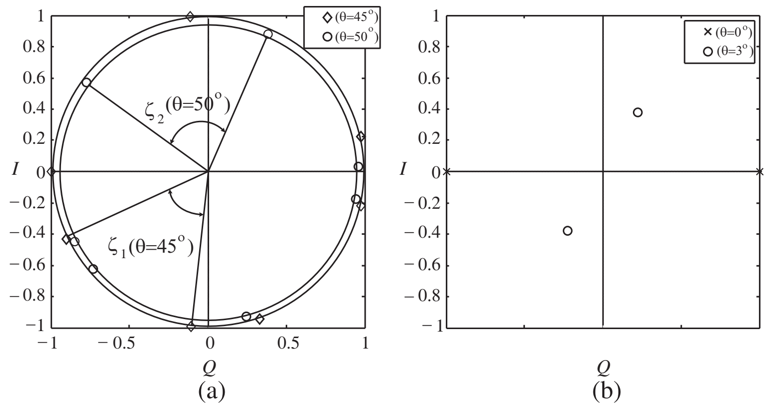

Figure 5. Constellation diagram of the RF directional modulation signal. (a) Communication and direction-finding application. (b) Secure communication application.

angle information of the receiver is modulated into the transmit signal constellation. Figure 5 shows the constellation diagram of the RF directional modulation signal used for physical layer secure communication application and communication and direction-finding application, respectively. For the physical layer secure communication application, the constellation diagram of the RF directional modulation signal is the same as the traditional BPSK modulation signal when the receiver at the desired direction ($\theta = 0^\circ$), while the constellation points become distorted when the receiver is out of the desired direction ($\theta = 3^\circ$). For the communication and direction-finding application, the constellation diagram of the RF directional modulation signal is scrambled when the receiver at the desired range. However, the total phase value of this scrambled constellation diagram is a function of the azimuth angle information. Determining how to extract the data information and azimuth angle information from this scrambled constellation diagram is a crucial problem. A data information demodulation algorithm and an azimuth angle information estimation algorithm will be presented in Sections 3 and 4, respectively.

2.3. Frequency-domain Analysis

Consider that the amplitude spectrum of the excitation signal $s(t)$ is denoted by $E(j\omega)$ with modulation bandwidth $2\omega_b$. The spectrum function of the switching function is a series of impulse function, which appears at different harmonic frequencies because the switching function $U_m(t)$ is a periodic function. The expression of the spectrum function is written as:

$$S(j\omega) = \sum_{i=-\infty}^{i=+\infty} \pi \dot{A}_i \delta(\omega - i\omega_p) \tag{8}$$

$$\dot{A}_i = \frac{2\tau}{T} Sa\left(\frac{i\omega_p \tau}{2}\right) \tag{9}$$

$$\omega_p = 2\pi f_p = \frac{2\pi}{T} \tag{10}$$

where $\dot{A}_i$ denotes the amplitude of the ith harmonic component, and ω_p denotes the switching angular frequency and $Sa(x) = \frac{\sin x}{x}$. According to the convolution theorem in frequency-domain and Equation (3), the receive signal in frequency-domain can be expressed as follows:

$$R(j\omega) = \frac{1}{2\pi} E(j\omega) * S(j\omega) = \frac{\tau}{T} \sum_{i=-\infty}^{i=+\infty} Sa\left(\frac{i\omega_p \tau}{2}\right) E[j(\omega - i\omega_p)] \tag{11}$$

The amplitude spectrum of the RF directional modulation signal due to the switching function is illustrated in Figure 6, which is a repetition of the modulation spectrum centered at the carrier radian frequency ω_0. The envelope of the harmonic components follows the function $Sa(x)$, which is determined from the Fourier transform of the switching function. The amplitude spectrum of the RF directional modulation signal not only appears at the carrier radian frequency ω_0 (fundamental component) but also removes the fundamental component to the radian frequencies $\omega_0 \pm \omega_p$, $\omega_0 \pm 2\omega_p$, $\ldots$, and $\omega_0 \pm i\omega_p$ (harmonic components), respectively, unlike using a single antenna to radiate BPSK modulation signal directly. Figure 7 shows the power of fundamental and harmonic components for the RF directional modulation signal alone with $M = 7$, $M = 15$ and $M = 31$, respectively. Compared with the power level of the BPSK modulation signal transmitted by a single antenna array (regarded as 0 dB), the power level of the fundamental component reduces to

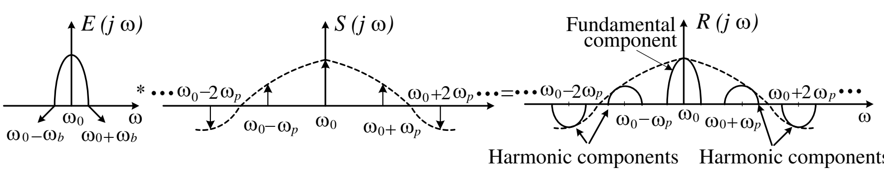

Figure 6. The amplitude spectrum of the receive signal.

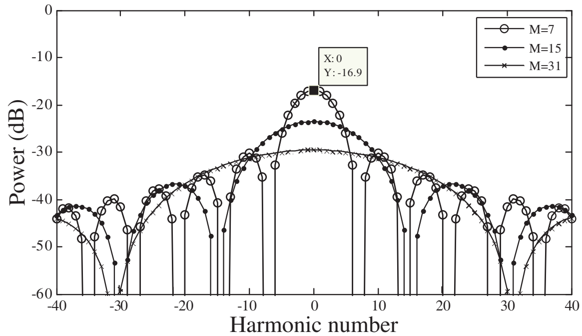

Figure 7. The power of the fundamental and harmonic components.

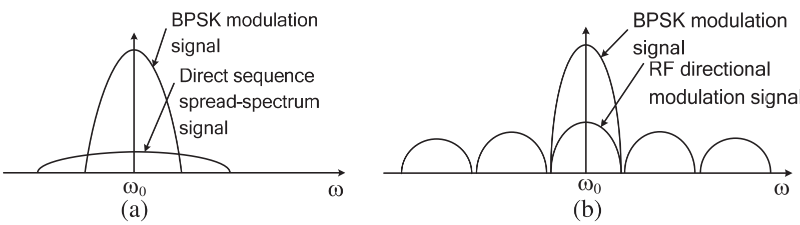

Figure 8. Comparison diagram of the power spectrum between the direct sequence spread-spectrum signal and the RF directional modulation signal. (a) Spread spectrum using direct sequence. (b) Spread spectrum using a switched antenna array.

-16.9 dB, and the total bandwidth is spreading when $M = 7$. This power spectrum characteristic is similar to traditional direct sequence spread-spectrum signal. Figure 8 shows the comparison diagram of the spread-spectrum between the direct sequence spread-spectrum signal and the RF directional modulation signal. The RF directional modulation signal is formed by switching the antenna array, unlike the direct sequence spread-spectrum signal which mixes the data with a spreading sequence directly before the final carrier modulation.

3. DIFFERENTIAL CORRELATED DEMODULATION ALGORITHM OF THE DATA INFORMATION

From the principle of RF directional modulation technique, we can find that the RF directional modulation signal is similar to the traditional direct sequence spread-spectrum signal at the frequency-domain. However, the phase center locus of the RF directional modulation signal varies with the azimuth angle for communication and direction-finding application unlike physical layer secure communication application, which only needs to correlate the receive signal with the spreading sequence. This traditional demodulation algorithm of the direct sequence spread-spectrum signal is not suitable for the RF directional modulation signal of this paper. Therefore, we employ a differential correlated demodulation algorithm to demodulate the data information. Consider that the receive signal goes through power amplifier, down converter and sampling device. Then, the baseband signal is obtained and denoted by $R(kT_\Omega)$ where $f_\Omega = \frac{1}{T_\Omega} = Mf_p$ denotes the sampling frequency, and k denotes kth sampling point. According to the maximum likelihood principle, the data information can be estimated as follows:

$$e^{j\hat{b}_n\pi} = \sum_{k=1}^{M} \frac{R(nM+k)R^*\left[(n-1)M+k\right]}{R\left[(n-1)M+k\right]R^*\left[(n-1)M+k\right]},\ n = 2, 3, \ldots, N \quad (12)$$

where the superscript $(\bullet)^*$ denotes the complex conjugate of a matrix. Then the data information $\hat{b}_n$ can be obtained by a BPSK decision device.

4. AZIMUTH ANGLE ESTIMATION ALGORITHM

From Equations (5)–(7), an azimuth angle estimation algorithm is developed as follows:

Step 1: calculate the phase difference between two adjacent sampling points by Equation (13).

$$\varphi_{k,k+1} = angle\left[\frac{r(kT+T)}{r(kT)}\right],\ k = 1, 2, \ldots, M-1 \quad (13)$$

Step 2: change principal value region. When $\varphi_{k,k+1} > 0$, $\varphi_{k,k+1} = \varphi_{k,k+1}$, and when $\varphi_{k,k+1} < 0$, $\varphi_{k,k+1} = \varphi_{k,k+1} + 2\pi$.

Step 3: extract the Doppler frequency shift information from the baseband signal by Equation (14) as follows:

$$\hat{f}_d = \frac{1}{2\pi}\sum_{k=1}^{M-1}\left\{\varphi_{k,k+1} + floor\left[\frac{1}{2}V\cos\left(\frac{\theta_1+\theta_2}{2}\right)\right]\right\}f_p \quad (14)$$

Step 4: estimate the azimuth angle from the Doppler frequency shift information by Equation (15) as follows:

$$\hat{\theta} = a\cos\left[\frac{2\hat{f}_d}{(M-1)Vf_p}\right] \quad (15)$$

5. SIMULATION RESULTS

The simulation conditions are supposed as follows:

(1) The switching frequency f_p equals 10 MHz; the number of element in each antenna cluster V equals 5; the desired receiver is at the range of $[40^{\circ}, 50^{\circ}]$; each frame signal contains $N = 100$ BPSK modulation symbols. It is noted that the receiver cumulates one frame receive signal to estimate the azimuth angle in simulation.

(2) The transmit signal at $\theta = 45^{\circ}$ (mainlobe direction) as standard signal is used to calculate the adding power of AWGN. For other directions, the adding power of AWGN is the same as the direction $\theta = 45^{\circ}$. It means that the added power of AWGN is the same at the desired range $[40^{\circ}, 50^{\circ}]$.

(3) Simply for expression, the RF directional modulation technique for communication and direction-finding application is expressed as application 1, and the RF directional modulation technique for physical layer secure communication is expressed as application 2 in simulation.

Figure 9 shows the bit-error-ratio (BER) performances versus signal-to-noise ratio (SNR) when $M = 7$ and the receiver at different directions. For application 2, the BER performance is the same as traditional BPSK direct sequence spread-spectrum signal when the receiver is at the desired direction $\theta = 0^{\circ}$, while the RF directional modulation signal cannot be demodulated when the receiver is out of the desired direction. It means that the RF directional modulation signal can obtain $10 \times \log_{10}(M) = 8.45$ dB spread-spectrum gain

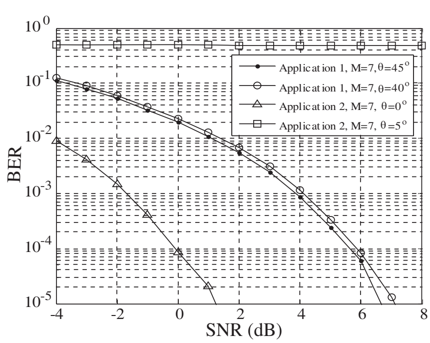

Figure 9. BER performance versus SNR when $M = 7$ and the receiver at the different directions.

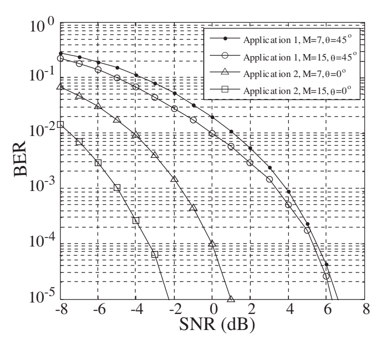

Figure 10. BER performance versus SNR when $M = 7$ and $M = 15$, respectively.

at the desired direction. For application 1, the BER performances have a little difference when the receiver at the directions $\theta = 40^{\circ}$ and $\theta = 45^{\circ}$ because the receive signal power is different at these directions in the beam space. However, the RF directional modulation signal only obtains about 2.4 dB spread-spectrum gain unlike the RF directional modulation signal for application 2, which can obtain full spread-spectrum gain as traditional BPSK direct sequence spread-spectrum signal. Figure 10 shows the BER performance versus SNR when $M = 7$ and $M = 15$, respectively. We can find that the RF directional modulation signal for application 2 can obtain 8.45 dB and 11.76 dB spread-spectrum gain, respectively, as traditional BPSK direct sequence spread-spectrum signal, while the spread-spectrum gain improves hardly with the M increasing. Although the BER performance at the desired range $[40^{\circ}, 50^{\circ}]$ for application 1 is less than the BER performance at the desired direction $\theta = 0°$ for application 2, the RF directional modulation signal for application 1 can realize direction-finding function.

Figure 11 shows the root mean square error (RMSE) performance of the azimuth angle versus azimuth angle when SNR equals to 15 dB and $M = 7$. We can find that the RMSE performance achieves about 0.01 degree when the receiver is at the desired range $[40^{\circ}, 50^{\circ}]$. Figure 12 shows the RMSE performance versus SNR when the receiver is at the direction $\theta = 47^{\circ}$ and $M = 7$. The curve shows that the RMSE performance improves with the SNR increasing obviously. Figure 13 shows the RMSE performance versus the transmit antenna group M when the receiver is at the direction $\theta = 47^{\circ}$ and when SNR equals 10 dB. Although the BER performance of application 2 improves hardly with the transmit antenna cluster M increasing, the direction-finding performance improves obviously.

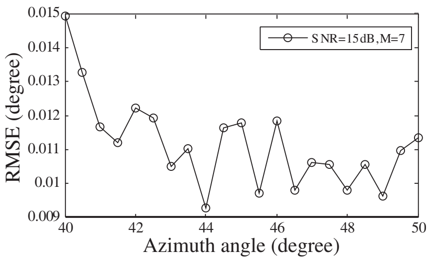

Figure 11. RMSE performance versus azimuth angle when SNR equals to 15 dB and $M = 7$.

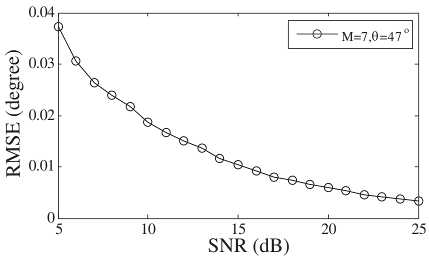

Figure 12. RMSE performance versus SNR when the receiver at the direction $\theta = 47^{\circ}$ and $M = 7$.

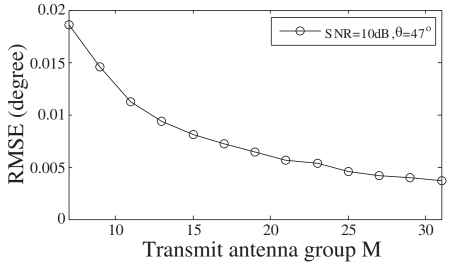

Figure 13. RMSE performance versus M when the receiver at the direction $\theta = 47^\circ$ and SNR equals to 10 dB.

6. CONCLUSION

Traditionally, RF directional modulation technique is used for physical layer secure communication, which causes the transmit signal's constellation scrambled at undesired directions. However, we propose a RF directional modulation technique using a switched antenna array for communication and direction-finding applications in this paper, which demodulates the data information and the directional information into the transmit signal constellation. In this way, a receiver with a single antenna can demodulate the data information and azimuth angle information from the scrambled constellation simultaneously. This RF directional modulation technique offers a comprehensive scheme for communication and direction-finding from the point of view of RF modulation technique. Therefore, the proposed signal of this paper can be applied to the system such as communication and tracking systems, radar, navigation systems and guidance beacon because the transmit signal constellation contains the data information and spatial parameters. However, the RF directional modulation signal for communication and direction-finding application cannot obtain full spread-spectrum gain compared with the RF directional modulation signal for the physical layer secure communication. Future work on the problem such as improving the spread-spectrum gain of the RF directional modulation signal for communication and direction-finding application is required.

ACKNOWLEDGMENT

This work was supported by the Aeronautic Science Foundation of China under Grant No. 20095152026, and by the Natural Science Foundation of Jiangsu Province under Grant No. BK2009367.

REFERENCES

1. Daly, M. P. and J. T. Bernhard, "Directional modulation technique for phased arrays," *IEEE Transactions on Antennas and Propagation*, Vol. 57, No. 9, 2633–2640, 2009.
2. Daly, M. P., E. L. Daly, and J. T. Bernhard, "Demonstration of directional modulation using a phased array," *IEEE Transactions on Antennas and Propagation*, Vol. 58, No. 5, 1545–1550, 2010.
3. Daly, M. P. and J. T. Bernhard, "Beamsteering in pattern reconfigurable arrays using directional modulation," *IEEE Transactions on Antennas and Propagation*, Vol. 58, No. 7, 2259–2265, 2010.
4. Babakhani, A., D. B. Rutledge, and A. Hajimiri, "Transmitter architectures based on near-field direct antenna modulation," *IEEE Journal of Solid-State Circuits*, Vol. 43, No. 12, 2674–2692, 2008.
5. Hong, T., M.-Z. Song, and Y. Liu, "RF directional modulation technique using a switched antenna array for physical layer secure communication applications," *Progress In Electromagnetics Research*, Vol. 116, 363–379, 2011.
6. Song, M. Z. and T. Hong, "Microwave space modulation carrying azimuth and elevation transmitted by monopulse antenna," *Journal of Electromagnetic Waves and Applications*, Vol. 22, Nos. 2–3, 277–289, 2008.
7. Hong, T., M.-Z. Song, and X.-Y. Sun, "Design of a sparse antenna array for communication and direction finding applications based on the chinese remainder theorem," *Progress In Electromagnetics Research*, Vol. 98, 119–136, 2009.
8. Jacobs, E. W., D. W. Fogliatti, H. Nguyen, D. J. Albares, C. T. Chang, and C. K. Sun, "Photo-injection p-i-n diode switch for high-power RF switching," *IEEE Transactions on Microwave Theory and Techniques*, Vol. 50, No. 2, 413–419, 2002.
9. Chou, H. T., K. L. Hung, and C. Y. Chen, "Utilization of a Yagi antenna director array to synthesize a shaped radiation pattern for optimum coverage in wireless communications," *Journal of Electromagnetic Waves and Applications*, Vol. 23, No. 7, 851–861, 2009.
10. Kazemi, S., F. Keshmiri, and H. R. Hassani, "Amplitude distribution synthesize of unequally spaced arrays," *Journal of Electromagnetic Waves and Applications*, Vol. 23, Nos. 8–9, 987–997, 2009.

11. He, Q.-Q., H.-D. He, and H. Lan, "An efficient pattern synthesis method for cylindrical phased array antennas," *Journal of Electromagnetic Waves and Applications*, Vol. 23, No. 4, 473–482, 2009.
12. Lim, S.-H., J.-H. Han, S.-Y. Kim, and N.-H. Myung, "Azimuth beam pattern synthesis for airborne SAR system optimization," *Progress In Electromagnetics Research*, Vol. 106, 295–309, 2010.
13. Shanks, H. E. and R. W. Bickmore, "Four-dimensional electromagnetic radiators," *Canad. J. Phys.*, Vol. 37, 263–275, Mar. 1959.
14. Yang, S., Y. B. Gan, and P. K. Tan, "A new technique for power-pattern synthesis in time-modulated linear arrays," *IEEE Antennas Wireless Propag. Lett.*, Vol. 2, 285–287, 2003.
15. Aksoy, E. and E. Afacan, "Thinned nonuniform amplitude time-modulated linear arrays," *IEEE Antennas Wireless Propag. Lett.*, Vol. 9, 514–517, 2010.
16. Pal, S., S. Das, and A. Basak, "Design of time-modulated linear arrays with a multi-objective optimization approach," *Progress In Electromagnetics Research B*, Vol. 23, 83–107, 2010.
17. Poli, L., P. Rocca, L. Manica, and A. Massa, "Pattern synthesis in time-modulated linear arrays through pulse shifting," *IET Microw. Antennas Propag.*, Vol. 4, No. 9, 1157–1164, 2010.
18. Yang, S., Y. B. Gan, A. Qing, and P. K. Tan, "Design of a uniform amplitude time modulated linear array with optimized time sequences," *IEEE Transactions on Antennas and Propagation*, Vol. 53, No. 7, 2337–2339, Jul. 2005.
19. Li, G., S. Yang, M. Huang, and Z. Nie, "Sidelobe suppression in time modulated linear arrays with unequal element spacing," *Journal of Electromagnetic Waves and Applications*, Vol. 24, Nos. 5–6, 775–783, 2010.
20. Yang, S., Y. Chen, and Z.-P. Nie, "Simulation of time modulated linear antenna arrays using the FDTD method," *Progress In Electromagnetics Research*, Vol. 98, 175–190, 2009.
21. Yang, S., Y. B. Gan, and P. K. Tan, "Linear antenna arrays with bidirectional phase center motion," *IEEE Transactions on Antennas and Propagation*, Vol. 53, No. 5, 1829–1835, May 2005.
22. Yang, S., Y. B. Gan, and A. Qing, "Moving phase center antenna arrays with optimized static excitations," *Microw. Opt. Technol. Lett.*, Vol. 38, No. 1, 83–85, Jul. 2003.
23. Yang, S., Y. B. Gan, and P. K. Tan, "Comparative study of low sidelobe time modulated linear arrays with different time

schemes," *Journal of Electromagnetic Waves and Applications*, Vol. 18, No. 11, 1443–1458, 2004.

24. Li, G., S. Yang, and Z. Nie, "A study on the application of time modulated antenna arrays to airborne pulsed Doppler radar," *IEEE Transactions on Antennas and Propagation*, Vol. 57, No. 5, 1578–1582, May 2009.
25. Li, G., S. Yang, and Z. Nie, "Direction of arrival estimation in time modulated linear arrays with unidirectional phase center motion," *IEEE Transactions on Antennas and Propagation*, Vol. 58, No. 4, 1105–1111, 2010.
26. Fondevila, J., J. C. Brégains, F. Ares, and E. Moreno, "Application of time modulation in the synthesis of sum and difference patterns by using linear arrays," *Microw. Opt. Tech. Lett.*, Vol. 48, No. 5, 829–832, May 2006.
27. Rocca, P., L. Manica, L. Poli, and A. Massa, "Synthesis of compromise sum-difference arrays through time-modulation," *IET Radar Sonar Navig.*, Vol. 3, No. 6, 630–637, Nov. 2009.
28. Fredrick, J. D., Y. X. Wang, S.-S. Jeon, and T. Itoh, "A Smart antenna receiver array using a single RF channel and digital beamforming," *IEEE MTT-S International Microwave Symposium Digest*, Vol. 1, 311–314, 2002.
29. Bregains, J. C., J. Fondevila-Gomez, G. Franceschetti, and F. Ares, "Signal radiation and power losses of time-modulated arrays," *IEEE Transactions on Antennas and Propagation*, Vol. 56, No. 6, 1799–1804, 2008.
30. Yang, S., Y. B. Gan, and A. Qing, "Sideband suppression in time-modulated linear arrays by the differential evolution algorithm," *IEEE Antennas Wireless Propag. Lett.*, Vol. 1, 173–175, 2002.
31. Tong, Y. Z. and A. Tennant, "Reduced sideband levels in time-modulated arrays using half-power sub-arraying techniques," *IEEE Transactions on Antennas and Propagation*, Vol. 59, No. 1, 301–303, 2011.
32. Poli, L., P. Rocca, L. Manica, and A. Massa, "Time modulated planar arrays — Analysis and optimisation of the sideband radiations," *IET Microw. Antennas Propag.*, Vol. 4, No. 9, 1165–1171, 2010.
33. Rocca, P., L. Poli, G. Oliveri, and A. Massa, "Synthesis of time-modulated planar array with controlled harmonic radiations," *Journal of Electromagnetic Waves and Applications*, Vol. 24, Nos. 5–6, 827–838, 2010.

34. Poli, L., P. Rocca, L. Manica, and A. Massa, "Handling sideband radiations in time-modulated arrays through particle swarm optimization," *IEEE Transactions on Antennas and Propagation*, Vol. 58, No. 4, 1408–1411, 2010.
35. Tennant, A., "Experimental two-element time-modulation direction finding array," *IEEE Transactions on Antennas and Propagation*, Vol. 58, No. 3, 986–988, 2010.
36. Tennant, A. and B. Chambers, "A two-element time-modulated array with direction-finding properties," *IEEE Antennas Wireless Propag. Lett.*, Vol. 6, 64–65, 2007.
37. Li, G., S. Yang, Y. Chen, and Z.-P. Nie, "A novel electronic beam steering technique in time modulated antenna arrays," *Progress In Electromagnetics Research*, Vol. 97, 391–405, 2009.
38. Tong, Y. and A. Tennant, "Simultaneous control of sidelobe level and harmonic beam steering in time-modulated linear arrays," *Electron. Lett.*, Vol. 46, No. 3, Feb. 2010.
39. Poli, L., P. Rocca, G. Oliveri, and A. Massa, "Harmonic beamforming in time-modulated linear arrays," *IEEE Transactions on Antennas and Propagation*, Vol. 59, No. 7, 2538–2545, Jul. 2011.
40. Dimousios, T. D., C. D. Nikolopoulos, S. A. Mitilineos, and C. N. Capsalis, "A new low-profile and cost SPA-PIFA for mobile 2.4 GHz ISM applications," *Journal of Electromagnetic Waves and Applications*, Vol. 24, No. 7, 881–891, 2010.
41. Viani, F., L. Lizzi, M. Donelli, D. Pregnolato, G. Oliveri, and A. Massa, "Exploitation of parasitic smart antennas in wireless sensor networks," *Journal of Electromagnetic Waves and Applications*, Vol. 24, No. 7, 993–1003, 2010.
42. Soltani, S., M.-N. Azarmanesh, E. Valikhanloo, and P. Lotfi, "Design of a simple single-feed dual-orthogonal-linearly-polarized slot antenna for concurrent 3.5 GHz WIMAX and 5 GHz WLAN access point," *Journal of Electromagnetic Waves and Applications*, Vol. 24, No. 13, 1741–1750, 2010.